JOURNAL OF COMPUTATIONAL PHYSICS 104, 23–29 (1993)

Numerical Study of a Singular Differential Equation Relevant for the Finite β Tearing Mode in a Toroidal Plasma*

M. S. CHU, J. M. GREENE, M. KLASKY,† AND M. S. CHANCE‡

General Atomics, San Diego, California 92186-9784

Received October 16, 1990; revised August 21, 1991

The generalized Green's function method proposed by Miller and Dewar (*J. Comput. Phys.* **66**, 356 (1986)) and Pletzer and Dewar in *Computational Techniques & Applications: CTAC-89, Proceedings, Int. Conf. Brisbane, 1989*, edited by W. L. Hogarth and B. J. Noye, in press, for solving the singular differential equation occurring in the finite β tearing mode problem has been tested numerically on a model differential equation. This method is compatible with a variational formulation of the problem and gives accurate numerical answers with high powers of convergence with respect to the number of grid points used. When the method is extended to the more physically relevant two-sided problem at moderate pressure gradients, a less stringent condition on the Frobenius expansion is required because the principal value of the otherwise divergent integrals associated with the method is shown to exist.

I. INTRODUCTION

The central numerical problem of importance in the finite β tearing mode in a toroidal plasma [3] is modeled on the solution of the differential equation

$$\mathscr{L}y=\left[\frac{d^2}{dx^2}-\frac{g(x)}{x^2}\right]y=0, \tag{1}$$

near its singular point $x=0$. In (1)

$$g(x)=\sum_{i=0}^{\infty}x^i g_i \tag{2}$$

is the power series expansion of $g(x)$ with g_i the coefficient of the ith power of x. The singular behavior is affected most by the values of g_0 and g_1; y is the perturbed flux function, x is the equilibrium flux function label, and g_0 is related to the magnetic well depth. (1) is defined between $x=\pm 1$, with $x=0$ being the location of the mode singular surface, and $x=\pm 1$, the location of external conducting boundaries. It is easy to write down the general Frobenius expansion of the solution to (1) near $x=0$,

$$y=|x|^{\alpha}\sum_{j=0}^{\infty}a_j x^j. \tag{3}$$

The coefficient a_j of the $(j+\alpha)$th power of x is given by the recurrence relation

$$a_j=\left(\sum_{m=1}^{j}g_m a_{j-m}\right)\Big/[(\alpha+j)(\alpha+j-1)-g_0], \qquad j=1,2,\ldots. \tag{4}$$

The indicial equation $\alpha(\alpha-1)-g_0=0$ determines two values for

$$\alpha=\tfrac{1}{2}\mp\mu, \tag{5}$$

where

$$\mu=(g_0+\tfrac{1}{4})^{1/2}. \tag{6}$$

The interesting case for a tokamak is $g_0>0$, so we assume $\mu>\frac{1}{2}$. The α's in turn, determine the large and small solutions for y

$$y_{\mathrm{L}}=|x|^{1/2-\mu}[1+a_{1\mathrm{L}}x+\cdots+a_{j\mathrm{L}}x^j+\cdots], \tag{7}$$

and

$$y_{\mathrm{S}}=|x|^{1/2+\mu}[1+a_{1\mathrm{S}}x+\cdots]. \tag{8}$$

* This is a report of work sponsored by the U.S. Department of Energy under Contracts DE-AC03-89ER53277 and DE-AC02-76-CHO-3073.

† Rensselaer Polytechnic Institute, Troy, New York 12181-2000.

‡ Princeton Plasma Physics Laboratory, Princeton, New Jersey 08543.

0021-9991/93 $5.00

The solution of the numerical problem is thus reduced to finding the value of Δ, such that

$$y = y_L + \Delta y_S \tag{9}$$

satisfies the boundary condition $y = 0$ at $x = \pm 1$.

Much former numerical work has been expended on finding Δ. One of the methods relies on a complicated sequence of convergence studies by using a sequence of finite elements to extract Δ [4]. The other one involves the shooting method [5], starting from $x = 1$, relying on integrating the solutions accurately toward $x = 0$ to extract the functional dependence of y, and the value of Δ from y_L and y_S. These have been known to be satisfactory in one-dimensional problems where an extremely fine or adaptive mesh is easily implemented, but a straightforward extension to situations suitable for the two-dimensional problem is unclear.

An alternative method (generalized Green's function) has recently been proposed by Miller and Dewar [1] and Pletzer and Dewar [2]. It also utilizes the known behavior of (7) and (8) near $x = 0$ and expresses Δ as an integral of the solutions. Due to the fact that Δ is expressed as an integral, this method is expected to be superior.

It is the purpose of this note to substantiate the findings of Refs. [1, 2] and report that the method is directly applicable to possible situations arising from the finite β tearing mode in a tokamak.

In the next section, the method is described with emphasis on the one-sided problem, i.e., $0 < x \leqslant 1$, the results of which are presented in Section III. In the real physical situation, the two-sided problem is more relevant. For this case, we have found that because of the existence of the principal values of the integrals involved in the method, we can relax the constraints on the number of terms required in the Frobenius expansion. The results showing this are described in Section IV.

II. DESCRIPTION OF THE METHOD

To begin, the solution y is decomposed as $y \equiv y_0 + y_1$, where y_1 is chosen as a sum of an n term truncated representation of y_L given by (7) and y_D

$$y_1 = y_L + y_D. \tag{10}$$

The component y_D is $o(x^{\mu + 1/2})$ or, explicitly,

$$y_D = x^h + a_{D1} x^{h+1} + \cdots. \tag{11}$$

It represents the "deviation" of y_1 from y_L, and h is required to be larger than $\mu + \frac{1}{2}$, so that the deviation is smaller than the small solution near $x = 0$. y_1 is also required to satisfy the boundary condition

$$y_1(1) = 0. \tag{12}$$

With y_1 thus specified, y_0 is determined by the relationship

$$\mathscr{L} y_0 = -\mathscr{L} y_1, \tag{13}$$

with the boundary conditions

$$y_0(0) = y_0(1) = 0. \tag{14}$$

This is usually accomplished variationally by using a galerkin expansion of y_0 and taking the appropriate inner product of y_0 with (13). The coefficient Δ of the small solution y_S can then be expressed as convergent integrals of y_0 and y_1. This relationship is easily derivable starting from

$$\begin{aligned} 0 &= \int_0^1 (y_0 + y_1)\, \mathscr{L}(y_0 + y_1)\, dx \\ &= \int_0^1 y_0 \mathscr{L} y_0\, dx + \int_0^1 y_1 \mathscr{L} y_0\, dx \\ &\quad + \int_0^1 y_0 \mathscr{L} y_1\, dx + \int_0^1 y_1 \mathscr{L} y_1\, dx. \end{aligned}$$

We note that

$$\int_0^1 y_1 \mathscr{L} y_0\, dx - \int_0^1 y_0 \mathscr{L} y_1\, dx = -2\mu\Delta, \tag{15}$$

so Δ can be written in the form

$$\mu\Delta(a, b) = I_1(a, b) + I_2(a, b) - I_3(a, b), \tag{16}$$

with $a = 0$, $b = 1$ for the one-sided problem. In (16),

$$I_1(a, b) = \frac{1}{2} \int_a^b y_1 \mathscr{L} y_1\, dx, \tag{17}$$

$$I_2(a, b) = \int_a^b y_0 \mathscr{L} y_1\, dx, \tag{18}$$

$$I_3(a, b) = \frac{1}{2} \int_a^b \left[\left(\frac{dy_0}{dx} \right)^2 + \frac{g}{x^2} y_0^2 \right] dx. \tag{19}$$

It is easy to verify that Δ given by (16) is variational with respect to y_0 with (13) as its Euler equation for the eigenfunction y_0. Furthermore, (16) is invariant to the choice of y_D so long as $h > \mu + \frac{1}{2}$. The variational expression given by (16) is a desirable form to be used for the tearing mode study because, in this case, I_3 corresponds to δW and $\mathscr{L}$

corresponds to the Euler equation operator [6]. Both δW and $\mathscr{L}$ are important concepts in magnetohydrodynamics.

So far in the formulation of the model problem, we have tacitly assumed that the expansion in (2) for $g(x)$ and consequently the expansions (7) and (8) for y_L and y_S are known accurately to arbitrary powers in x near $x=0$. In practice, this is known, with a reasonable effort, only to a few terms. Thus, one of the purposes of our study is to determine and verify numerically how many terms in the expansion are needed. It is clear from the definition (17) that I_1 is defined if $\mathscr{L}y_1$ vanishes at 1 to a sufficiently high power in x. This means that the Frobenius expansion (7) for y_L has to be carried out to sufficiently high order. For a given μ, this puts the number of terms required to be $n > 2\mu$; i.e., $n=2$, for $\frac{1}{2} < \mu < 1$ or $0 < g < 0.75$; $n=3$, for $1 < \mu < \frac{3}{2}$ or $0.75 < g < 1.25$; etc.

To anticipate situations which might arise in the finite β tearing mode in which multiple singular surfaces may arise, say at $x=a<1$, we modify y_D so that

$$y_1(x)=0 \qquad \text{for} \quad a<x<1. \tag{20}$$

III. NUMERICAL TESTS—THE ONE-SIDED PROBLEM

A finite element computer program employing Hermite cubics [7] has been constructed to solve the variational problem for Δ. Three-point Gaussian integration was used for the evaluation of the coefficient matrix in the variational problem and the integrals I_1, I_2, I_3. Mesh accumulation is arranged by taking the mesh points x_i to be given by

$$x_i=(i-1)^{\alpha}\,\delta x. \tag{21}$$

Due to the fact that for the small solution

$$\frac{dy_S}{dx}=\left(\mu+\frac{1}{2}\right)x^{\mu-1/2}+\cdots, \tag{22}$$

and hence $(dy_S/dx)|_{x=0}=0$ for $\mu > \frac{1}{2}$, it is then possible to put

$$\left.\frac{dy_S}{dx}\right|_{x=0}=0, \tag{23}$$

as a boundary condition on dy_S/dx, in addition to the other two boundary conditions given in (14). From (13), it is easy to show that the solution y_0 to (13) gives $I_2=2I_3$. This relationship is verified to the roundoff accuracy of the computation, which is 10^{-12} to 10^{-13}. The requirement (20) demands $x=a$ to be treated as an internal boundary point. Since $\mathscr{L}$ is a second-order differential operator, we also required

$$\left.\frac{dy_1}{dx}\right|_{x=a}=0. \tag{24}$$

In the following, we present three essential classes of examples of the results for (16) derived from the numerical solutions of (13) and compare these with the exact closed form analytic solutions of (1).

Case 1. $g=g_0$. In this case, a family of possible analytic solution satisfying all the above requirements is given by

$$y_1=\begin{cases} x^{1/2-\mu}-\dfrac{(1+\gamma_1 x)}{(1+\gamma_1 a)}\,a^{1/2-\mu-h}x^h, & x<a, \\ 0, & x>a; \end{cases} \tag{25}$$

$$y_0=\begin{cases} \dfrac{(1+\gamma_1 x)}{(1+\gamma_1 a)}\,a^{1/2-\mu-h}x^h-x^{1/2+\mu}, & x<a, \\ x^{1/2-\mu}-x^{1/2+\mu}, & x>a, \end{cases} \tag{26}$$

with

$$\gamma_1 a=\frac{1-2\mu-2h}{1+2\mu+2h} \tag{27}$$

and

$$\Delta_1^{\mathrm{Ana}}=-1. \tag{28}$$

This case corresponds to $j=\infty$ in (7). Equation (16) converges for $h>\mu+\frac{1}{2}$. It is also possible to give analytic expressions to all the quantities I_1, I_2, I_3 in the model. In general, it is found that a small number of grid points ($N\sim 50$) is sufficient to give accurate solutions of y_0 and dy_0/dx. Due to the fast variation of y_0 and dy_0/dx near $x=0$, it is found that a high degree of grid packing [8] is needed for the convergence of these quantities. As has been estimated in Ref. [8], grid packing leads to convergence in y_0 as N^{-4} and dy_0/dx as N^{-3}. Here we emphasize the convergence of the quantities I_1, I_2, and I_3. We have not been able to obtain a good analytic estimate of the convergence rate of these quantities. Numerically, they have been found to converge at the rate of N^{-6}. For instance, with $N=81$, $g_0=0.25$, $\alpha=4$, $h=2.0$, $a=0.5$, the numerical solution y_0 deviates from (26) by less than 2×10^{-7} and dy_0/dx deviates from (27) by less than 5×10^{-3} everywhere. The maximum error occurs near $x=0$. Shown in Fig. 1 is the relative error

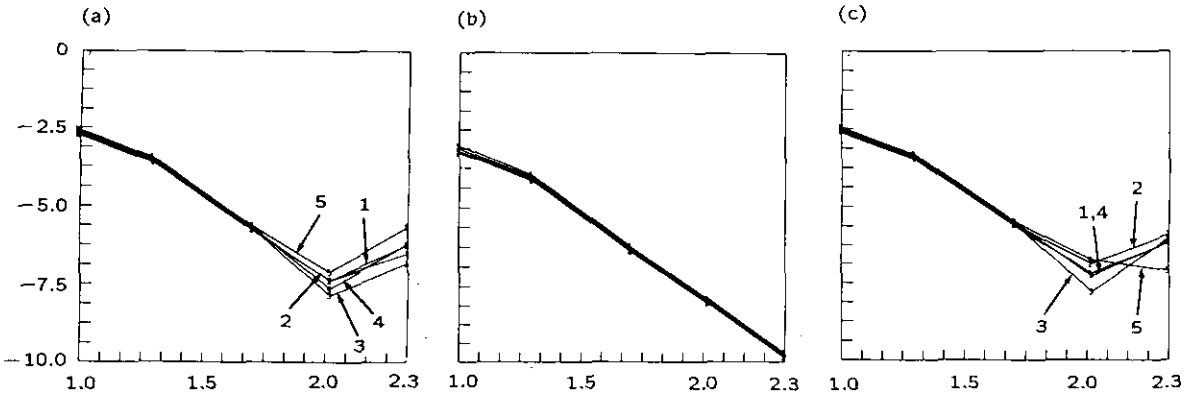

FIG. 1. Plot of the magnitude of (a) relative total error, (b) relative I_1 error, and (c) relative I_2 error in y_0 as a function of number of grid points N employed in the numerical computation for Case 1 in the text. $\alpha = 4$, $h = 3.5$, and $a = 0.5$. The value of g_0 for curve 1 is 0.01; 2, 0.19; 3, 0.37; 4, 0.56; and 5, 0.74. The analytic value for Δ is -1 independent of g_0. Note that the abscissa and the ordinate are on $\log_{10}$ scale.

for Δ, $\mathscr{E}_\Delta = (|\Delta_1^{\text{Num}} - \Delta_1^{\text{Ana}}|)/|\Delta^{\text{Ana}}|$; the relative error in I_1, $\mathscr{E}_{I_1} = (|I_1^{\text{Num}} - I_1^{\text{Ana}}|)/|\Delta^{\text{Ana}}|$; and the relative error in I_2, $\mathscr{E}_{I_2} = (|I_2^{\text{Num}} - I_2^{\text{Ana}}|)/|\Delta^{\text{Ana}}|$ for $a = 0.5$, $\alpha = 4$, $h = 3.5$, with various values of g_0 as a function of the number of grid points used. We note that, although I_1 may be integrated to better accuracy than that shown here, three-point Gaussian quadrature gives sufficient accuracy for our purpose. This is a desirable situation for finite element application of the present method using Hermite cubic elements. Note that the plot is on a $\log_{10}$ versus $\log_{10}$ scale. The maximum number of grid points used is 200. It is clearly seen that the errors all scaled as N^{-6}. In this example, $\mathscr{E}_{I_2}$, and consequently $\mathscr{E}_\Delta$, reduces until the number of grid points reaches 100 and then increases due to truncation error coming in from the numerical evaluation of other quantities such as $y_{2\mu}$ and $\Gamma(2\mu)$. This is checked by increasing the grid points beyond 200 and observing that the error further increases. With a larger value of the arbitrary internal point a, the errors are substantially reduced. We note that the condition (24) is necessary. If it is not imposed, a large error occurs in dy_0/dx and in all the other quantities.

Case 2. $g = g_0 - x$. This case also allows an easy complete analytic solution,

$$y_1 = \begin{cases} x^{1/2-\mu} - \dfrac{x^{3/2-\mu}}{1-2\mu} - \left(\dfrac{1+\gamma x}{1+\gamma a}\right) \\ \qquad \times a^{1/2-\mu-h}\left(1 - \dfrac{a}{1-2\mu}\right) x^h, \quad x < a, \\ 0, \qquad x > a; \end{cases} \tag{29}$$

$$y_0 = \begin{cases} \dfrac{\sqrt{x}\,\pi}{\Gamma(2\mu)}\left[\dfrac{Y_{2\mu}(2)}{J_{2\mu}(2)} J_{2\mu}(2\sqrt{x}) - Y_{2\mu}(2\sqrt{x})\right] \\ \qquad - x^{1/2-\mu} + \dfrac{1}{1-2\mu} x^{3/2-\mu} \\ \qquad + \left(\dfrac{1+\gamma_2 x}{1+\gamma_2 a}\right) a^{1/2-\mu-h} \\ \qquad \times \left(1 - \dfrac{a}{1-2\mu}\right) x^h, \quad x < a, \\ \dfrac{\sqrt{x}\,\pi}{\Gamma(2\mu)}\left[\dfrac{Y_{2\mu}(2)}{J_{2\mu}(2)} J_{2\mu}(2\sqrt{x}) - Y_{2\mu}(2\sqrt{x})\right], \quad x > a, \end{cases} \tag{30}$$

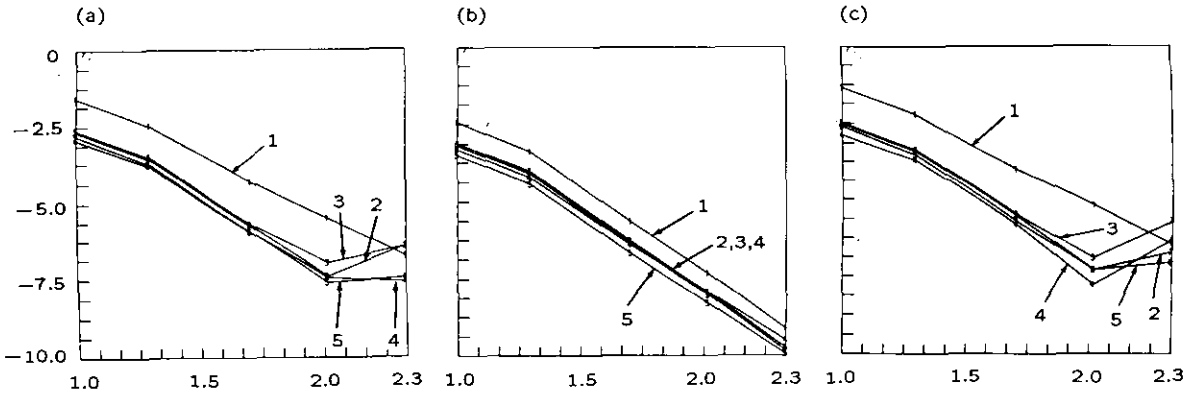

FIG. 2. Plot of the magnitude of (a) relative total error, (b) relative I_1 error, and (c) relative I_2 error in y_0 as a function of number of grid points N employed in the numerical computation for Case 2 in the text. In this example, $\alpha = 4$, $h = 3.5$, and $a = 0.5$. The value of g_0 for curve 1 is 0.01; 2, 0.17; 3, 0.35; 4, 0.62; and 5, 0.74. The analytic value for Δ is given in Eq. (32). Note that the abscissa and the ordinate are on $\log_{10}$ scale.

with

$$\gamma_2 a = \frac{(1-2\mu)(1-2\mu-2h)-a(3-2\mu-2h)}{(1-2\mu)(1+2\mu+2h)-a(2h+2\mu-1)} \tag{31}$$

and

$$\Delta_2^{\text{Ana}} = \frac{\pi}{2\Gamma(2\mu)^2}\left[\frac{Y_{2\mu}(2)}{J_{2\mu}(2)} - \frac{\cos(2\mu\pi)}{\sin(2\mu\pi)}\right], \tag{32}$$

for taking two terms in (7) for y_L and a correspondingly more complicated expression when three terms are adopted. As discussed before, with two terms, the method guarantees convergent results for $0.5 < \mu < 1$. We have verified numerically that this is true. The only complication arises in the evaluation of I_1 using the three-point Gaussian integration, due to the nearly divergent behavior of its integrand. This is not expected to give rise to difficulty because the analytic value for I_1 is known there. Again, in this case, grid packing is necessary to guarantee good convergence. And, a two-term representation for y_0 gives virtually identical values for I_2 and I_3 as the three-term representation. Therefore, we have verified that for $0 < g < 0.75$ values, we need to know the solution to y_1 only to two-term accuracy. Shown in Fig. 2 are the relative errors in $\mathscr{E}_\Delta$, $\mathscr{E}_{I_1}$, and $\mathscr{E}_{I_2}$ as a function of N with $\alpha = 4$, $h = 3.5$, and $a = 0.5$ for various values of g_0. It is seen that we again obtain N^{-6} convergence.

Case 3. $g = g_0 + x$. For completeness, we list the analytic solution for this case

$$y_1 = \begin{cases} x^{1/2-\mu} + \dfrac{x^{3/2-\mu}}{1-2\mu} - \left(\dfrac{1+\gamma x}{1+\gamma a}\right) \\ \qquad \times a^{1/2-\mu-h}\left(1+\dfrac{a}{1-2\mu}\right)x^h, \quad x < a, \\ 0, \quad x > a; \end{cases} \tag{33}$$

$$y_0 = \begin{cases} \dfrac{\sqrt{x}\,2}{\Gamma(2\mu)}\left[K_{2\mu}(2\sqrt{x}) - \dfrac{K_{2\mu}(2)}{I_{2\mu}(2)} I_{2\mu}(2\sqrt{x})\right] - x^{1/2-\mu} \\ \qquad - \dfrac{1}{1-2\mu} x^{3/2-\mu} \\ \qquad + \left(\dfrac{1+\gamma x}{1+\gamma a}\right) a^{1/2-\mu-h} x^h, \quad x < a, \\ \dfrac{2\sqrt{x}}{\Gamma(2\mu)}\left[K_{2\mu}(2\sqrt{x}) - \dfrac{K_{2\mu}(2)}{I_{2\mu}(2)} I_{2\mu}(2\sqrt{x})\right], \quad x > a, \end{cases} \tag{34}$$

with

$$\gamma_3 a = \frac{(1-2\mu)(1-2\mu-2h)+a(3-2\mu-2h)}{(1-2\mu)(1+2\mu+2h)+a(2h+2\mu-1)} \tag{35}$$

and

$$\Delta_3^{\text{Ana}} = -\frac{1}{\mu[\Gamma(2\mu)]^2}\left[\frac{K_{2\mu}(2)}{I_{2\mu}(2)} + \frac{\pi}{2\sin(2\mu\pi)}\right]. \tag{36}$$

The behavior of the numerical solution for this case parallels the previous two cases with similar error and grid convergence properties. We emphasize here that the errors shown in Figs. 1a and 2a are partly due to the errors in I_1. I_1 can, in general, be written in terms of exactly known functions. Their errors can, therefore, be eliminated and the errors in Δ reduced to those coming from I_2 and I_3 only.

IV. EXTENSION TO THE TWO-SIDED PROBLEM

An interesting extension of the above discussion is provided by the situation in which Eq. (1) is defined over the interval $(-1, 1)$, and the final desired answer is $\Delta(-1, 1)$. In this case we note that we may define

$$\Delta(-1, 1) = \lim_{\varepsilon \to 0} [\Delta(-1, -\varepsilon) + \Delta(\varepsilon, 1)]. \tag{37}$$

Consider the following expression for $\mathscr{L}y_1$, where y_1 is a series of the form of Eq. (7):

$$\begin{aligned} \mathscr{L}y_1 = &- |x|^{-3/2-\mu}\left[g_0 + \tfrac{1}{4} - \mu^2\right] \\ &- |x|^{-1/2-\mu}(\operatorname{sgn} x)\{a_{1L}[g_0 - (\tfrac{3}{2}-\mu)(\tfrac{1}{2}-\mu)] + g_1\} \\ &- |x|^{1/2-\mu}\{a_{2L}[g_0 - (\tfrac{5}{2}-\mu)(\tfrac{3}{2}-\mu)] + a_{1L} g_1 + g_2\} \\ &- \cdots. \end{aligned} \tag{38}$$

Condition (6) eliminates the first term in (38). In the examples in Section II, the second term is eliminated by the choice of

$$a_{1L} = \frac{g_1}{1-2\mu}. \tag{39}$$

The resultant integral I_1 would then be convergent if $\mu < 1$ or $g_0 < \frac{3}{4}$. In the present situation, we keep only one term in the Frobenius expansion by setting $a_{1L} = 0$, the leading term in $I_1(-a, -\varepsilon) + I_1(\varepsilon, b)$ is then given by

$$I_1(-a, -\varepsilon) + I_1(\varepsilon, b) = \int_{-a}^{-\varepsilon} |x|^{-2\mu} g_1 \, dx - \int_{\varepsilon}^{b} g_1 |x|^{-2\mu} \, dx, \tag{40}$$

$$= g_1 \frac{a^{1-2\mu} - b^{1-2\mu}}{(1-2\mu)}, \tag{41}$$

an answer independent of ε; i.e., the principal value exists.

Note, however, that when only one term from y_L in (7) is included in y_1, then the rest of the terms in (7) manifest themselves in y_0. This changes the leading behavior in y_0 to be $a_{1L}x^{3/2-\mu}$ and, in the one-sided problem, gives rise to a divergent contribution to (15), which was used inobtaining relation (16). However, it is easy to show that this divergent contribution cancels exactly in (37). Further, we may verify that the other integrals involved in the calculation of (37) all converge. For this case, (16) remains intact when the principal value evaluation of (37) is employed. Thus, we would expect that only one term in the Frobenius expansion is sufficient for $0 < g_0 < \frac{3}{4}$ or $\frac{1}{2} < \mu < 1$.

Since Case 3 is the reflection through the origin of Case 2, we combined them and modified (29) and (33) to their corresponding expression for one term in the Frobenius expansion. In this case, the analytical value of Δ is given by

$$\Delta(-1, 1) = \Delta_2^{\text{Ana}} + \Delta_3^{\text{Ana}}. \tag{42}$$

To study the numerical behavior of $\Delta(-1, 1)$, the straightforward Hermite cubics [7] are not sufficiently accurate for representing y_0 in (13). We modified the Hermite cubics of the first interval centered at x_2 to be

$$\begin{aligned}\psi_I(x) &= \frac{1}{(2\mu-1)}\left[\left(\frac{1}{2}+\mu\right)\left(\frac{x}{x_2}\right)^{3/2-\mu} - \left(\frac{3}{2}-\mu\right)\left(\frac{x}{x_2}\right)^{1/2+\mu}\right], \quad 0 < x < x_2, \\ \omega_I(x) &= \frac{x_2}{1-2\mu}\left[\left(\frac{x}{x_2}\right)^{3/2-\mu} - \left(\frac{x}{x_2}\right)^{1/2+\mu}\right], \\ & \qquad 0 < x < x_2.\end{aligned} \tag{43}$$

Note that $\psi_I(x_2) = 1$, $\psi_I'(x_2) = 0$, and $\omega_I(x_2) = 0$, $\omega_I'(x_2) = 1$. So, these elements join smoothly to the right-hand side of the ordinary Hermite cubics. The resultant behavior of the relative error in Δ versus grid points is plotted in Fig. 3 for different values of $g_0 = 0.01$, 0.19, 0.37, 0.57, and 0.74. We note that, in this two-sided problem, I_1 is formally divergent. To display clearly the errors coming from I_2 and I_3, the analytic expression for the principal value integral of I_1 is used in Δ. For further application of the method in which analytic principal value of the integral of I_1 is not readily available, a numerical integration scheme for finding the principal value with errors smaller than those displayed for Δ in Fig. 3 is called for. It is seen that the errors are uniformly small even for a relatively small number of grid points used, although the grid point convergence scales only like N^{-1}. When nonuniform grid is used, the error turns out to be larger than uniform grid. We conclude that for μ in the range $\frac{1}{2} < \mu < 1$, sufficient accuracy may be obtained for $\Delta(-1, 1)$ by using only one term in the Frobenius expansion for y_1. We note in passing that this phenomenon also manifests itself in the shooting method described in Ref. [5] for the one-dimensional problem, provided that the proper limits are observed at the singularity. This could prove to be of practical importance when the Frobenius expansion involves complicated operators like the 2D finite β tearing mode problem.

V. CONCLUSIONS

In conclusion, we have found that the generalized Green's function method proposed by Dewar *et al.* [1, 2] allows a variational formulation of the tearing mode problem in finite β. With sufficiently high grid packing factor $\alpha \simeq 4$, the method is accurate. The requirement of internal boundary points increases the magnitude of the relative error but keeps the correct scaling with the grid number to N^{-6}. For the range of $0 < g_0 < 0.75$, only one term in the Frobenius expansion is needed when only the sum of the Δ from both sides of the singularity is desired.

We note, in particular, the generalized Green's function method, by matching the large "trial function" to the large solution with sufficient accuracy near the singularity, renders the final answers in terms of convergent integrals of the solutions over the entire interval. For 2D problems, this is superior to the method used in Ref. [4], where only the finite element closest to the singular surface is forced to match to the large solution, resulting in numerical difficulty.

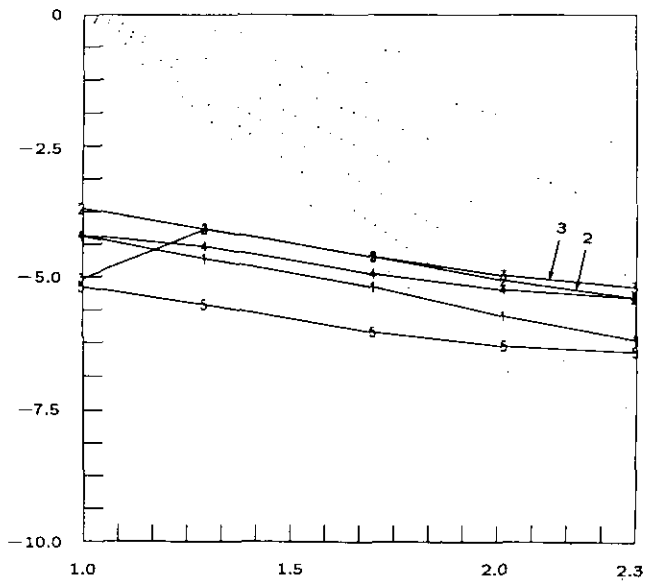

FIG. 3. Plot of the magnitude of the relative error in the sum of Δ defined in Eq. (37) as a function of the number of grid points N employed in the numerical computation described in Section III in the text. In this example, $\alpha = 1$, $h = 3.5$, and $a = 0.75$. The value of g_0 for curve 1 is 0.01; 2, 0.17; 3, 0.35; 4, 0.62; and 5, 0.74. The analytic value for Δ is given in Eq. (42). Note that the abscissa and the ordinate are on $\log_{10}$ scale.

It is also instructive to compare the generalized Green's function method with the method used in Ref. [5]. The two methods are similar at the start. Both methods seek to understand the analytic behavior of the large and small solutions by performing Frobenius expansion of the equations. The difference lies in the utility of this analytic information in the two methods. The method in Ref. [5] then went on to use purely numerical means to extract the coefficients of both the large and small solutions. An adaptive grid in the radial direction (excluding the singular point!), was actually required to obtain these coefficients. In the generalized Green's function method, the analytic development is carried further. The analytic behavior of the singular solutions was used and folded into numerically convergent integrals covering the whole radial interval. Only the small solution needs to be handled explicitly by numerical means. We regard these conceptual features in the generalized Green's function method superior to that given in Ref. [5]. These are explicitly relevant in 2D situations. The major difficulty in extending the generalized Green's function method to 2D is that the analytic pre-development of the theory leading to the large solution could be quite formidable.

REFERENCES

1. A. D. Miller and R. L. Dewar, *J. Comput. Phys.* **66**, 356 (1986).
2. A. Pletzer and R. L. Dewar, in *Computational Techniques & Applications: CTAC-89, Proceedings, Int. Conf. Brisbane, 1989*, edited by W. L. Hogarth and B. J. Noye, in press.
3. R. L. Dewar and R. G. Grimm, in *Singular Finite Element Methods in Plasma Stability Computations—a Simple Model, in Computational Techniques and Applications: CTAC-83*, edited by B. J. Noye and C. Fletcher (North Holland, Amsterdam, 1984), p. 730.
4. R. C. Grimm, R. L. Dewar, J. Manickam, S. C. Jardin, A. H. Glasser, and M. S. Chance, in *Plasma Physics and Controlled Fusion Research, Proceedings, 9th Int. Conf., Baltimore, 1982* (IAEA, Vienna, 1983), Vol. 3, p. 35.
5. M. S. Chance, H. P. Furth, A. H. Glasser, and H. Selberg, *Nucl. Fusion* **22**, 187 (1982).
6. M. S. Chu, M. S. Chance, J. M. Greene, and T. H. Jensen, *Phys. Fluids B* **2**, 97 (1990).
7. G. Strang and G. J. Fix, *An Analysis of the Finite Element Method* (Prentice–Hall, Englewood Cliffs, NJ, 1973).
8. G. Sewell, *The Numerical Solution of Ordinary Partial Differential Equations* (Academic Press, San Diego, 1988), p. 209.